





ARTICLE

<https://doi.org/10.1038/s41467-020-19517-y>

OPEN

Direct conversion of methane to formaldehyde and CO on B₂O₃ catalysts

Jinshu Tian^{1,3}, Jiangqiao Tan^{1,3}, Zhaoxia Zhang^{1,3}, Peijie Han¹, Min Yin¹, Shaolong Wan¹, Jingdong Lin¹, Shuai Wang¹   & Yong Wang²  

Direct oxidation of methane to value-added C₁ chemicals (e.g. HCHO and CO) provides a promising way to utilize natural gas sources under relatively mild conditions. Such conversions remain, however, a key selectivity challenge, resulting from the facile formation of undesired fully-oxidized CO₂. Here we show that B₂O₃-based catalysts are selective in the direct conversion of methane to HCHO and CO (~94% selectivity with a HCHO/CO ratio of ~1 at 6% conversion) and highly stable (over 100 hour time-on-stream operation) conducted in a fixed-bed reactor (550 °C, 100 kPa, space velocity 4650 mL g_{cat}⁻¹ h⁻¹). Combined catalyst characterization, kinetic studies, and isotopic labeling experiments unveil that molecular O₂ bonded to tri-coordinated BO₃ centers on B₂O₃ surfaces acts as a judicious oxidant for methane activation with mitigated CO₂ formation, even at high O₂/CH₄ ratios of the feed. These findings shed light on the great potential of designing innovative catalytic processes for the direct conversion of alkanes to fuels/chemicals.

¹State Key Laboratory for Physical Chemistry of Solid Surfaces, Collaborative Innovation Center of Chemistry for Energy Materials, National Engineering Laboratory for Green Chemical Productions of Alcohols-Ethers-Esters, and College of Chemistry and Chemical Engineering, Xiamen University, 361005 Xiamen, China. ²Voiland School of Chemical Engineering and Bioengineering, Washington State University, Pullman, WA 99164, USA. ³These authors contributed equally: Jinshu Tian, Jiangqiao Tan, Zhaoxia Zhang. ✉email: shuaiwang@xmu.edu.cn; yongwang@pnnl.gov

The catalytic transformation of methane to value-added chemicals is of significant interest for the efficient utilization of natural gas sources^{1,2}, especially due to the recent shale-gas revolution³. In particular, the direct conversion of methane via selective oxidation to C₁ chemicals (i.e. CH₃OH, HCHO, and CO) is most attractive, because all of these products are important platform molecules/intermediates for the production of fuels and chemicals^{4,5}. Selective oxidation of methane involves the cleavage of C–H bonds and formation of C–O bonds, leading to CH₃OH, HCHO, and CO as the desired partial oxidation products but also to CO₂ as an undesired complete oxidation product. Such oxidation processes are induced by nucleophilic attack of active O species at the H or C atom in CH₄ (or reactive intermediates) before electron transfer⁶. Because the desired C₁ partial oxidation products (i.e. CH₃OH, HCHO, and CO) have much higher electrophilicity than CH₄, they are kinetically more favored in oxidation, leading to dominant formation of undesired CO₂ at methane conversions even less than 5% on conventional catalysts^{7–12} (e.g., V₂O₅¹³, MoO₃¹⁴, and Fe₂O₃¹⁵). Lattice O anions exposed on these oxide surfaces act as the nucleophilic and oxidative centers that can be regenerated fast via dissociative adsorption of gaseous O₂ during catalytic cycles (also described as the Mars van Krevelen mechanism¹⁶). To our best knowledge, high selectivities to the desired C₁ partial oxidation products on these traditional metal oxide catalysts are able to be obtained merely at low methane conversions (<2%) or low O₂/CH₄ ratios (<0.5)^{7–15}, making such oxidation processes impractical.

Directly using molecular O₂ or derived O· radicals to oxidize CH₄, instead of the more nucleophilic and reactive lattice O anions, would render facile control over the extent of CH₄ oxidation. Recent studies^{17,18} have shown that nonmetallic B-based materials (e.g. BN^{19–21}, B₄C²², SiB₆²³, and B₂O₃^{24,25}) can catalyze oxidative dehydrogenation of C₂–C₄ alkanes to alkenes with extraordinarily low selectivities to CO₂, reflecting, in turn, that these catalysts probably use the moderate O₂ or O· oxidants to activate the alkane reactants. The BN catalyst has also been attempted for methane oxidation at temperatures above 690 °C, which yielded CO, CO₂, and methane coupling products (i.e. C₂H₄ and C₂H₆) with respective selectivities of 76.6, 4.3, and 19.3 at 20.5% methane conversion²⁶. We expect that the selectivity of valuable C₁ products for methane oxidation on the B-based

catalysts can be significantly improved at milder temperatures under which HCHO and CH₃OH can be better stabilized kinetically. Moreover, experiments of nuclear magnetic resonance spectroscopy²⁷ and X-ray photoelectron spectroscopy²² have revealed that B(OH)_xO_{3–x} (where $x = 0–3$) layers formed on the B-based catalysts act as the true active phase, irrespective of their bulk contents.

According to the above considerations, we here study supported B₂O₃ catalysts for selective methane oxidation at relatively mild temperatures. Our results show that B₂O₃-based catalysts are highly selective in the direct conversion of methane to HCHO and CO, and these selectivities are unexpectedly insensitive to the O₂/CH₄ ratios. Structural characterization, kinetic measurements, and isotopic labeling experiments are combined to discern that molecular O₂ bonded to coordinately unsaturated BO₃ centers on the B₂O₃ surfaces is the crucial oxidant that accounts for the selective methane oxidation. The mechanistic understanding of methane oxidation on the unique B₂O₃ surfaces would inspire the design of the next generation of heterogeneous catalysts for selective oxidation of hydrocarbons.

Results

Performances of B₂O₃-based catalysts in methane oxidation.

Catalysts containing 20 wt% B₂O₃ supported on various oxides (i.e. Al₂O₃, SiO₂, ZnO, TiO₂, and ZrO₂) were prepared using the wetness impregnation method with boric acid (H₃BO₃) as the boron source (see Methods section). This high B₂O₃ loading was chosen to ensure that multiple B₂O₃ layers were formed on each oxide support (Supplementary Table 1). Under the conditions studied (O₂/CH₄ ratio of 1.0 and 550 °C), these oxide supports themselves were inactive for methane activation, whereas all supported catalysts with 20 wt% B₂O₃ selectively converted methane to HCHO and CO (~94 % selectivity with a HCHO/CO ratio of ~1), together with a trace amount of desired CH₃OH and C₂ products (C₂H₄ and C₂H₆), which are irrespective of the nature of the support (Fig. 1a). It is noteworthy that these observed conversions are mainly attributed to the catalytic processes on the B₂O₃ surface, instead of gas-phase radical reactions, because the conversion and selectivity of methane oxidation on the supported B₂O₃ catalysts had negligible changes whether the empty space of the reactor was fully filled with inert SiC material or not (Supplementary Fig. 1) and their sum did not obey the

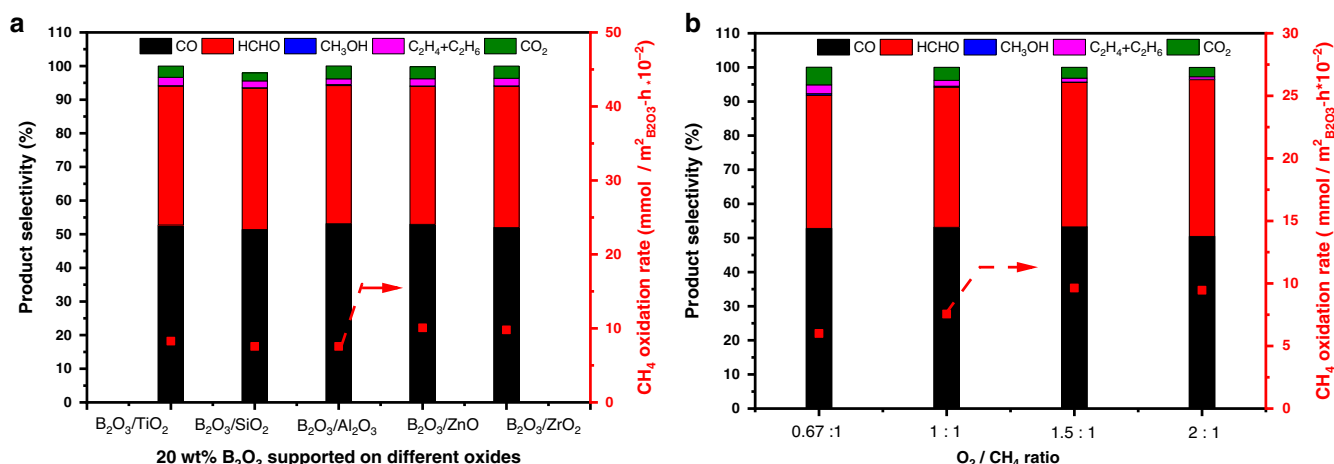


Fig. 1 Methane oxidation rates and selectivity on supported B₂O₃ catalysts. **a** Effects of oxide support on 20 wt% B₂O₃-based catalysts. **b** Effects of O₂/CH₄ ratio on 20 wt% B₂O₃/Al₂O₃. Reaction conditions: 550 °C, 32 kPa P_{CH₄}, 32 kPa P_{O₂} for **(a)** or 21–64 kPa P_{O₂} for **(b)**, gas composition balanced with N₂, ~6% CH₄ conversion was achieved by adjusting the space velocity within a range of 1500–50000 mL g_{cat}⁻¹ h⁻¹. The methane oxidation rates reported here were normalized by the exposed surface area of B₂O₃. The bars in **a** and **b** denote product selectivities (CO in black, HCHO in red, CH₃OH in blue, C₂H₄ and C₂H₆ in magenta, and CO₂ in green), and the red square in **a** and **b** denote methane oxidation rates.

empirical 100% rule²⁸ that was observed in the previous gas phase chemistry (Supplementary Fig. 2).

In all cases, the sum of the selectivities to these desired C_1 and C_2 products were above 96%, while the selectivity to undesired CO_2 was below 4% at ~6% methane conversion (controlled by the space velocity for rigorous selectivity comparison among the examined catalysts). Such high selectivities to the partial oxidation products reflect the superior control of the oxidation extent within the kinetic regime, brought forth by the unique property of the B_2O_3 -based catalysts as described below, otherwise the fully oxidized CO_2 would be predominant among the products if the thermodynamic equilibrium is established (e.g., 53.5% methane conversion and 72.8% CO_2 selectivity at 550 °C and 100 kPa with an initial CH_4/O_2 molar ratio of 1/1; Supplementary Fig. 3). This highly selective methane oxidation process could be scaled up by combining efficient separation of the products from the effluent and recycling of the unconverted CH_4 and O_2 reactants²⁹. Moreover, the fact that the molar ratio of HCHO to CO in the products is ~1.0 makes them potentially desired for the downstream acetic acid synthesis via hydrogenation of HCHO to methanol and its subsequent carbonylation^{30,31} and also for glycolic acid synthesis via direct carbonylation of HCHO³². The detected C_2H_6 and C_2H_4 products are likely ascribed to methane oxidative coupling as we reported previously^{21,26}, reflecting the ability of B_2O_3 -based catalysts to produce C_{2+} molecules from direct methane oxidation. Similar methane oxidation rates (mmol methane converted per surface area of the exposed B_2O_3 phase per hour) were obtained for the examined catalysts. These results suggest a negligible effect of the oxide supports on catalytic performance, a result that is consistent with formation of the multiple B_2O_3 layers on each oxide support at 20 wt% B_2O_3 loading (the loading threshold for forming a B_2O_3 monolayer for each of the oxide supports are shown in Supplementary Table 1).

We further studied the effects of O_2/CH_4 partial pressure ratios on the performances of the 20 wt% B_2O_3/Al_2O_3 catalyst at 550 °C, where methane conversions were kept ~6% via adjusting the space velocity for rigorous comparison of reactivity and selectivity. As shown in Fig. 1b, nearly constant selectivities (i.e., >95% selectivity to desired C_1 and C_2 products with <5% selectivity to undesired CO_2) were obtained at ~6% methane conversion over a wide range of P_{O_2}/P_{CH_4} ratios (0.67–2.00), reflective of the unique ability of B_2O_3 in preventing complete oxidation of the desired C_1 and C_2 products to CO_2 and thus the potential of high-pressure operation for this catalytic process. Such remarkable selectivities to the desired C_1 and C_2 products and a negligible effect of the P_{O_2}/P_{CH_4} ratio on activity makes this system superior to conventional oxide catalysts (e.g. supported V_2O_5 and MoO_3 in Supplementary Table 2), which must operate at much lower P_{O_2}/P_{CH_4} ratios (0.1–0.5) to minimize the over-oxidation of C_1 and C_2 products by the strongly nucleophilic lattice O anions on metal oxide surfaces^{16,33}. Figure 1b also shows that methane oxidation rates increased with increasing the O_2/CH_4 ratio, indicating a positive reaction order with respect to O_2 . In addition, these B_2O_3 -based catalysts exhibited exceptional stability at 550 °C as illustrated over 100 h time-on-stream stable methane oxidation for the B_2O_3/Al_2O_3 catalyst (Supplementary Fig. 4).

Active sites of B_2O_3 -based catalysts for methane oxidation. To provide insight into the nature of active sites on these supported B_2O_3 catalysts, ^{11}B solid state nuclear magnetic resonance (NMR) was used. Two boron oxide species with chemical shifts centered at 67.9 and 57.1 ppm were observed for these samples (using $NaBH_4$ as the reference compound, NMR spectra shown in

Supplementary Fig. 5). These are ascribed to tri-coordinated BO_3 and tetra-coordinated BO_4 units, respectively³⁴. Previous studies^{35,36} suggest that the BO_4 units are derived from the additional bonding of lattice O anions of the oxide support to the BO_3 units in B_2O_3 . The BO_4/BO_3 molar ratio of the supported B_2O_3 catalysts increased with increasing basic strength of the oxide support (e.g. 0.46 for B_2O_3/SiO_2 , 1.45 for B_2O_3/Al_2O_3 , and 1.65 for B_2O_3/ZrO_2 in Supplementary Fig. 5) that can be explained by increased coordination of the B center to more basic lattice O anions of the oxide support. On the other hand, these BO_4/BO_3 ratios did not affect the methane oxidation rates of the supported B_2O_3 catalysts that were almost identical when normalized by the exposed B_2O_3 surface area (Fig. 1a). These results might indicate that the BO_3 and BO_4 units have similar catalytic activities.

To further confirm or disapprove our hypothesis, B-substituted ZSM-5 zeolite (B-ZSM-5) was prepared, where the B atoms embedded in the silicate framework were all tetra-coordinated by lattice O anions as confirmed by the single chemical shift of B at 54.1 ppm (Supplementary Fig. S5)^{37,38}. Compared with the supported B_2O_3 catalysts (e.g., 20 wt% B_2O_3/Al_2O_3), the B-ZSM-5 sample showed negligible activity in catalyzing methane oxidation with near 45% selectivity to CO_2 (Supplementary Fig. 6). It is thus concluded that the BO_4 units with full coordination of B centers are catalytically inactive. The fact that the methane oxidation rates of the supported B_2O_3 catalysts are independent of the BO_4/BO_3 ratio measured by ^{11}B NMR is likely due to that NMR is a bulk technique and that the top layer B_2O_3 is not bonded to the oxygen anions of oxide supports on these catalysts with multilayered B_2O_3 , leading to exclusively active surface BO_3 units for methane oxidation.

Mechanism of methane oxidation on B_2O_3 -based catalysts.

Kinetic studies were carried out to provide molecular-level insights into the mechanism of methane activation on supported B_2O_3 catalysts. The conversion-selectivity relationship for methane oxidation on 20 wt% B_2O_3/Al_2O_3 (Supplementary Fig. 7) showed that the selectivities to HCHO and CH_3OH both monotonically decreased as the conversion of CH_4 increased from 2 to 10%, concomitant with increased selectivities to CO and CO_2 . These selectivity trends indicate that both HCHO and CH_3OH are primary products formed from methane conversion. It has been proposed that the initial activation of methane by active O species on oxide surfaces forms bonded methoxy intermediates (CH_3O) via cleaving a C–H bond in methane, which undergo further dehydrogenation to form HCHO or recombine the cleaved H atom to form CH_3OH ^{39,40}. On B_2O_3 surfaces, methane selective oxidation to HCHO is the predominant reaction channel for methane activation, as evidenced by the high HCHO/ CH_3OH selectivity ratios obtained at low methane conversions (e.g. ~17 at 2% conversion, Supplementary Fig. 7). The secondary dehydrogenation of HCHO leads to the formation of CO, whereas the CO_2 product comes from CO oxidation.

Figure 2a depicts that the methane oxidation rate increased with O_2 pressure (0–80 kPa; 550 °C), but the dependence became weaker at higher O_2 pressure that is indicative of higher O_2 coverages on the B_2O_3 surface. In contrast, the methane oxidation rate increased linearly with the CH_4 pressure in the same pressure range, suggesting that CH_4 barely adsorbs on the BO_3 sites during catalysis (Fig. 2b), which is consistent with the unfavorable adsorption of CH_4 on solid surfaces brought forth by its highly symmetrical geometry and weakly polarized C–H bonds¹¹. These effects of reactant concentrations on the oxidation rates are indicative of the Eley-Rideal mechanism⁴¹ on catalytic surfaces, in

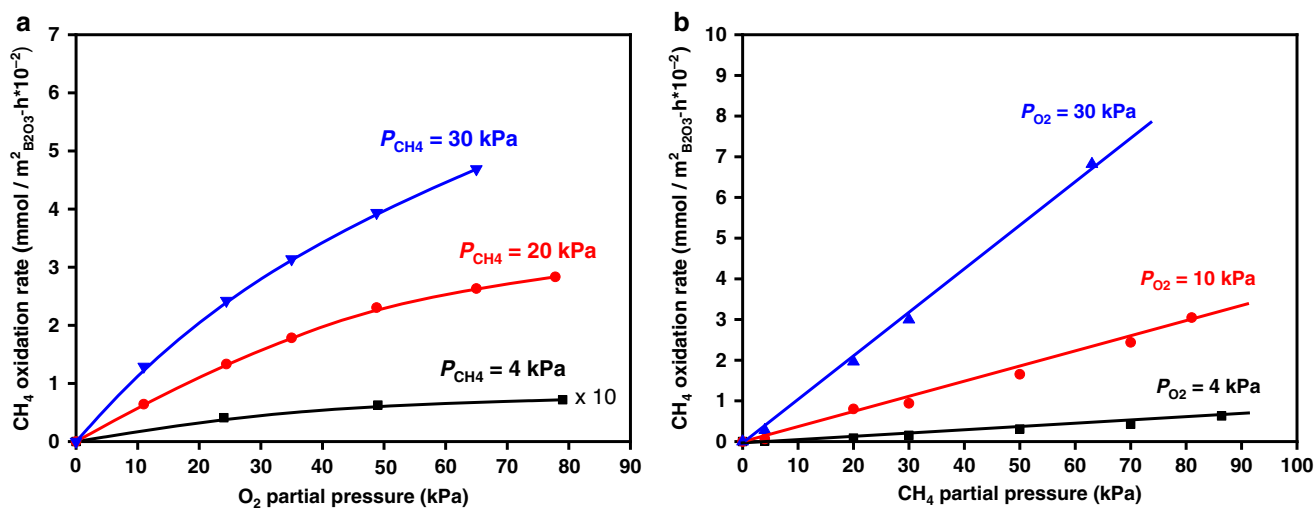


Fig. 2 Kinetics of methane oxidation on supported B_2O_3 catalysts. Methane oxidation rates as functions of **a** O_2 pressure and **b** CH_4 pressure were measured on 20 wt% B_2O_3/Al_2O_3 . Reaction condition: 550 °C, 4–30 kPa P_{CH_4} , 0–80 kPa P_{O_2} for **a** and 4–30 kPa P_{O_2} , 0–90 kPa P_{CH_4} for **b**, balanced by N_2 , space velocity at 4920 mL $g_{cat}^{-1} h^{-1}$. In **a**, the rate data measured at CH_4 partial pressures of 4, 20, and 30 kPa are shown as black square, red cycle, and blue triangle, respectively. In **b**, the rates measured at O_2 partial pressures of 4, 10, and 30 kPa were shown in black square, red cycle, and blue triangle, respectively. The curves in **a** and lines in **b** represent trends.

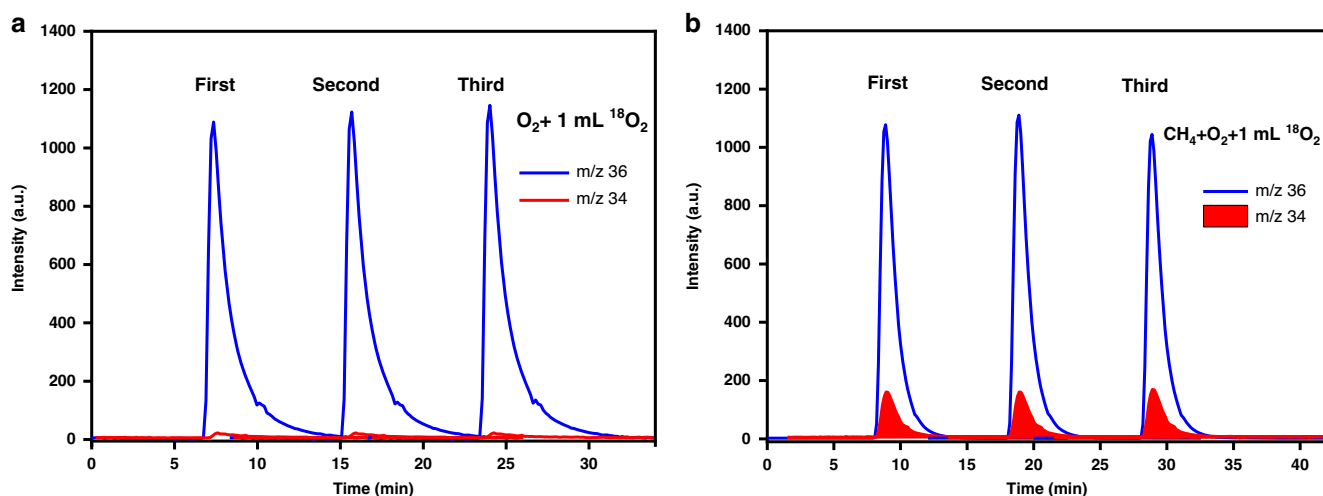


Fig. 3 Isotopic assessment of O_2 activation on supported B_2O_3 catalysts. Mass spectra of $^{16}O^{18}O$ ($m/z = 34$) species upon pulsing $^{18}O_2$ ($m/z = 36$) into $^{16}O_2$ flows on 20 wt% B_2O_3/Al_2O_3 were collected in the **a** absence and **b** presence of CH_4 (CH_4 1 mL/min, O_2 5 mL/min, N_2 4 mL/min, temperature: 550 °C, catalyst loading: 0.2 g). In both **a** and **b**, the red and blue curves denote the signals for the m/z ratios of 34 and 36, respectively.

which one molecule adsorbed on the active site directly reacts with another one from the gas phase. Because of this, we propose that methane oxidation occurs between a gaseous CH_4 molecule and an O_2 molecule bonded to the BO_3 sites. Similar Eley-Rideal-type pathways have been found for methane oxidation on Pd and Pt surfaces at high temperatures^{42,43}, which unveils that two adsorbed O atoms formed from the dissociation of a O_2 molecule on the catalyst surface are required to act concertedly in order to cleave the strong C–H bond of CH_4 .

Isotopic labeling experiments were further used to confirm the above hypothesis (i.e. BO_3 -surface-bonded O_2 directly activates CH_4). Pulses of a small amount of $^{18}O_2$ into flowing $^{16}O_2$ on the supported B_2O_3 catalysts at 550 °C did not lead to the formation of isotope-exchanged $^{18}O^{16}O$ species, excluding the presence of dissociative adsorption of O_2 molecules on the B_2O_3 surface (Fig. 3a). In contrast, when CH_4 was co-fed with $^{16}O_2$ and pulses of $^{18}O_2$ over the surface of the same B_2O_3 catalysts, a significant amount of $^{18}O^{16}O$ was detected (Fig. 3b). We thus infer that the

O–O bond in the adsorbed O_2 molecule is cleaved concertedly when it activates the C–H bond of CH_4 .

The above kinetic and isotopic assessments are combined to give a plausible pathway for the formation of HCHO from CH_4 oxidation on B_2O_3 -based catalysts as described in Fig. 4a. First, O_2 adsorbs on two vicinal BO_3 units with each O atom in O_2 bound to one of the electron-deficient B centers (Step 1, Fig. 4a). A gaseous CH_4 molecule then attacks this adsorbed O_2 reactant, resulting in concurrent formations of hydroxy and methoxy species (Step 2, Fig. 4a). Formaldehyde and H_2O are further produced from hydrogen abstraction of the methoxy moiety by a hydroxyl (Step 3, Fig. 4a). Desorption of these products from the active BO_3 sites completes a catalytic turnover for methane partial oxidation on B_2O_3 (Step 4, Fig. 3a). The measurable O-exchange between O_2 molecules in the presence of CH_4 (Fig. 3b) indicates the reversibility of Steps 1 and 2 on B_2O_3 under reaction conditions. This suggests, in turn, that Step 3 is kinetically relevant. This finding is consistent with a previous report⁶ that

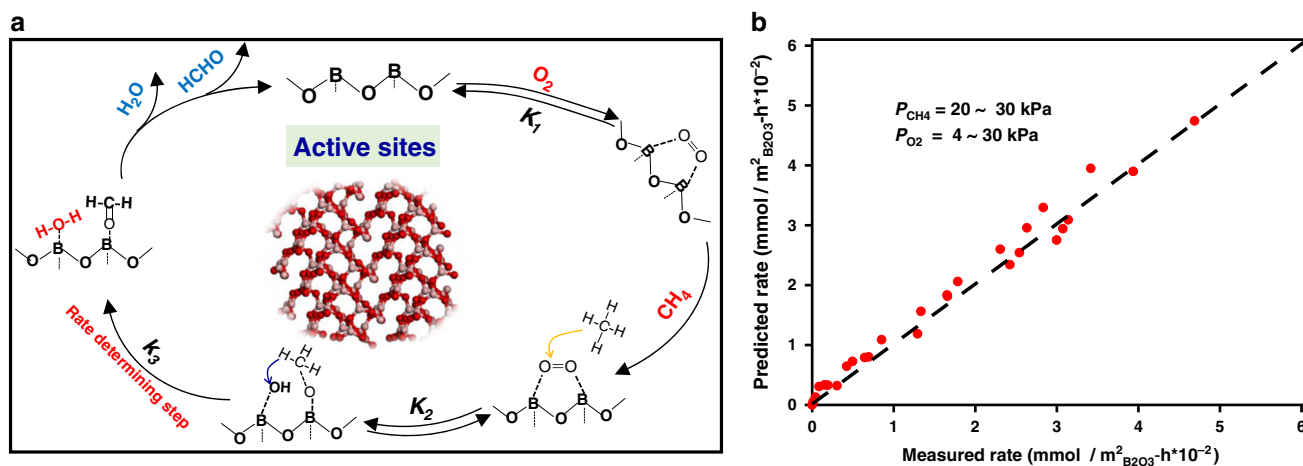


Fig. 4 Mechanistic insights for methane activation on a B_2O_3 surface. **a** Schematic diagram of the plausible pathway of methane selective oxidation to formaldehyde on B_2O_3 -based catalysts. **b** Parity plots for the measured rate data of methane selective oxidation on B_2O_3/Al_2O_3 and those predicted using Eq. 1 (the regression-fitted parameters shown in Supplementary Table 3). In **a**, K_1 and K_2 are equilibrium constants for the corresponding steps, and k_3 is the kinetic constant for hydrogen abstraction of the surface methoxy species by a neighboring hydroxyl.

the electronegativity of oxide catalysts affects the selectivity to HCHO. These elementary steps, taken together with the pseudo-steady-state approximation for all bound species and the quasi-equilibrated nature of all steps except Step 3, lead to an equation for methane conversion rates (r):

$$r = \frac{k_3 K_1 K_2 P_{O_2} P_{CH_4}}{1 + K_1 P_{O_2}} \quad (1)$$

Here, K_1 and K_2 are the respective equilibrium constants for Steps 1 and 2, whereas k_3 is the kinetic constant for Step 3. The functional form of Equation 1 accurately describes all methane oxidation rate data measured within a wide reactant pressure range (Fig. 4b; regression-fitted parameters shown in Supplementary Table 3), supporting the proposed methane activation mechanism on the B_2O_3 surfaces (Fig. 4a).

Discussion

In summary, nonmetallic B_2O_3 -based catalysts are selective and stable in the partial oxidation of methane to HCHO and CO. Surface tri-coordinated BO_3 units are the active sites for methane oxidation. O_2 molecules bound to the electron-deficient B centers of these BO_3 units are moderate oxidants for methane activation, exhibiting strong suppression of the formation of thermodynamically favored CO_2 . Further exploitation of such non-metallic oxide catalysts will bring innovative strategies and catalyst systems for efficient and selective oxidation of methane (and other alkanes) to valuable chemicals.

Methods

Preparation of B_2O_3 -based catalysts. B_2O_3 catalysts supported on various oxides (including Al_2O_3 , TiO_2 , ZnO , ZrO_2 , and SiO_2) were prepared by wetness impregnation method using boric acid (Sinopharm chemical reagent co. LTD) as the boron source. The preparation method was described below using B_2O_3/Al_2O_3 as an illustrative example: a certain amount of H_3BO_3 was dissolved in deionized water (10 mL) and then the resulting aqueous solution was added dropwise to pure Al_2O_3 (0.5 g). After stirring vigorously for 1 h, the impregnated samples were heated to 65 °C and subsequently vacuumed at 65 °C for 8 h. The as-prepared products were then calcined at 600 °C for 5 h in air.

Preparation of B-ZSM-5 samples. B-ZSM-5 was synthesized according to a previously reported method³⁷. Typically, NaOH, 1–6 hexanediamine (HMDA) and tetrapropylammonium bromide (TPABr) were dissolved in 18.9 mL of deionized water. The solution was stirred for 30 min, and then 1.8 g of porous SiO_2 (Aladdin) and 0.3373 g H_3BO_3 were slowly added. The gel was stirred for 1 h and then transferred into a teflon-lined stainless-steel autoclave for crystallization

at 180 °C for 48 h. The obtained samples were separated by filtration, washed with deionized water, dried at 90 °C for 12 h and finally calcined under static air at 550 °C for 5 h.

Measurement of catalytic performance. Catalytic methane oxidation was conducted using a fixed-bed quartz tubular reactor (7 mm inner diameter) with plug-flow hydrodynamics. The B_2O_3 -based catalyst (0.15–0.18 mm sieved particles, ~200 mg, corresponding to a volume of 0.38 mL) was first pretreated in flowing O_2/N_2 (1/1 in volume) for 2 h under 580 °C and then cooled to the reaction temperature under N_2 . CH_4/He (90/10%), O_2 (99.99%), and N_2 (99.99%) were individually controlled using three mass flow controllers (Sevenstar Technology Co., Ltd) to provide the reaction gas feed. The feed rate reported here is the weight hourly space velocity (WHSV), in which the gas volume refers to the standard ambient temperature and pressure. The concentrations of reaction products in the effluent were analyzed by an online gas chromatography (GC2060, Shanghai Ruimin GC Instruments, Inc). Samples in the quantitative ring were separated by Porapak column (6 m×3 mm) and then quantified using a thermal conductivity detector (TCD) for He, CH_4 , and CO_2 ⁴⁴. The other gases are introduced into a flame ionization detector (FID) and subsequently analyzed including CO, CH_4 , CO_2 , C_2H_4 , C_2H_6 , HCHO, and CH_3OH . Control experiments with SiC showed that there was negligible methane conversion without the catalyst. In all tests, carbon mass balances exceeded 98%. The CH_4 conversion (X_{CH_4}) and the carbon selectivity of each product i (S_i) were calculated using a standard normalization method (He as internal standard gas) based on the carbon balance, which were defined as

$$X_{CH_4} = \left(1 - \frac{P_{CH_4}^{out}}{P_{CH_4}^{in}}\right) \times 100\% \quad (2)$$

$$S_i = \frac{n_i P_i^{out}}{\sum n_i P_i^{out}} \times 100\% \quad (3)$$

Here, $P_{CH_4}^{out}$ and $P_{CH_4}^{in}$ are the corresponding partial pressures of methane at the outlet and inlet of the reactor, while P_i^{out} and n_i are the outlet partial pressure and the carbon number of each product i formed from methane oxidation, respectively.

Structural characterization. Specific surface areas of catalysts were measured by the Brunauer–Emmett–Teller (BET) method, using a Micromeritics Tristar 3020 surface area and porosimetry analyzer. Prior to measurement, all samples were degassed at 150 °C for 6 h. ^{11}B solid nuclear magnetic resonance (^{11}B -NMR) analysis was recorded on a Bruker NMR 500 DRX spectrometer at 500 MHz and referenced to $NaBH_4$ (3.2 ppm). Isotopic labeling experiments were performed in a fixed-bed single-pass flow micro-reactor. A mixture of N_2 and $^{16}O_2$ (research grade, 99.99%) was fed to the 20 wt% B_2O_3/Al_2O_3 catalyst bed at 550 °C until the baseline was stabilized and then an $^{18}O_2$ (Cambridge Isotope Lab., 99%; 1 mL each time) pulse was injected into the flow using a syringe. The chemical and isotopic compositions of the reactor effluent were measured by online mass spectrometry (MS, Pfeiffer, OminStar TM) at intervals of 10 s with a m/z scanning from 1 to 50. The m/z signals of 32, 34, and 36 represent $^{16}O^{16}O$, $^{16}O^{18}O$, and $^{18}O^{18}O$, respectively.

Data availability

The datasets generated and analyzed during the current study are available from the corresponding authors upon a reasonable request.

Received: 16 June 2020; Accepted: 8 October 2020;

Published online: 10 November 2020

References

- Agarwal, N. et al. Aqueous Au-Pd colloids catalyze selective CH₄ oxidation to CH₃OH with O₂ under mild conditions. *Science* **358**, 223–227 (2017).
- Marcinkowski, M. D. et al. H. Pt/Cu single-atom alloys as coke-resistant catalysts for efficient C-H activation. *Nat. Chem.* **10**, 325–332 (2018).
- Schwach, P., Pan, X. & Bao, X. Direct conversion of methane to value-added chemicals over heterogeneous catalysts: challenges and prospects. *Chem. Rev.* **117**, 8497–8520 (2017).
- Zhong, L. et al. Cobalt carbide nanoprisms for direct production of lower olefins from syngas. *Nature* **538**, 84–87 (2016).
- Jiao, F. et al. Selective conversion of syngas to light olefins. *Science* **351**, 1065–1068 (2016).
- Otsuka, K. & Hatano, M. The catalysts for the synthesis of formaldehyde by partial oxidation of methane. *J. Catal.* **108**, 252–255 (1987).
- Parmaliana, A. & Arena, F. Working mechanism of oxide catalysts in the partial oxidation of methane to formaldehyde. I. Catalytic behaviour of SiO₂, MoO₃/SiO₂, V₂O₅/SiO₂, TiO₂, and V₂O₅/TiO₂ systems. *J. Catal.* **167**, 57–65 (1997).
- Pitchai, R. & Klier, K. Partial oxidation of methane. *Catal. Rev. Sci. Eng.* **28**, 13–88 (1986).
- Mackie, J. C. Partial oxidation of methane: the role of the gas phase reactions. *Catal. Rev. Sci. Eng.* **33**, 169–240 (1991).
- Faraldos, M. et al. Comparison of silica-supported MoO₃ and V₂O₅ catalysts in the selective partial oxidation of methane. *J. Catal.* **160**, 214–221 (1996).
- Horn, R. & Schlögl, R. Methane activation by heterogeneous catalysis. *Catal. Lett.* **145**, 23–39 (2015).
- Fait, M. J. G. et al. Understanding trends in methane oxidation to formaldehyde: statistical analysis of literature data and based hereon experiments. *Catal. Sci. Technol.* **9**, 5111–5121 (2019).
- Berndt, H. et al. Structure and catalytic properties of VO_x/MCM materials for the partial oxidation of methane to formaldehyde. *J. Catal.* **191**, 384–400 (2000).
- Spencer, N. D. & Pereira, C. J. Partial oxidation of CH₄ to HCHO over a MoO₃-SiO₂ catalyst: A kinetic study. *AIChE J.* **33**, 1808–1812 (1987).
- Wang, Y. et al. SBA-15-supported iron phosphate catalyst for partial oxidation of methane to formaldehyde. *Catal. Today* **93–95**, 155–161 (2004).
- Chen, K., Khodakov, A., Yang, J., Bell, A. T. & Iglesia, E. Isotopic tracer and kinetic studies of oxidative dehydrogenation pathways on vanadium oxide catalysts. *J. Catal.* **186**, 325–333 (1999).
- Venegas, J. M., McDermott, W. P. & Hermans, I. Serendipity in catalysis research: Boron-based materials for alkane oxidative dehydrogenation. *Acc. Chem. Res.* **51**, 2556–2564 (2018).
- Shi, L. et al. Progress in selective oxidative dehydrogenation of light alkanes to olefins promoted by boron nitride catalysts. *Chem. Commun.* **54**, 10936–10946 (2018).
- Grant, J. T. et al. Selective oxidative dehydrogenation of propane to propene using boron nitride catalysts. *Science* **354**, 1570–1573 (2016).
- Shi, L. et al. Edge hydroxylated boron nitride for oxidative dehydrogenation of propane to propylene. *ChemCatChem* **9**, 1788–1793 (2017).
- Tian, J. et al. Propane oxidative dehydrogenation over highly selective hexagonal boron nitride catalysts: The role of oxidative coupling of methyl. *Sci. Adv.* **5**, eaav8063 (2019).
- Grant, J. T. et al. Boron and boron-containing catalysts for the oxidative dehydrogenation of propane. *ChemCatChem* **9**, 3623–3626 (2017).
- Yan, B., Li, W. C. & Lu, A. H. Metal-free silicon boride catalyst for oxidative dehydrogenation of light alkanes to olefins with high selectivity and stability. *J. Catal.* **369**, 296–301 (2019).
- Lu, W. D. et al. Supported boron oxide catalysts for selective and low-temperature oxidative dehydrogenation of propane. *ACS Catal.* **9**, 8263–8270 (2019).
- Love, A. M. et al. Synthesis and characterization of silica-supported boron oxide catalysts for the oxidative dehydrogenation of propane. *J. Phys. Chem. C* **123**, 27000–27011 (2019).
- Wang, Y. et al. Methane activation over a boron nitride catalyst driven by in situ formed molecular water. *Catal. Sci. Technol.* **8**, 2051–2055 (2018).
- Love, A. M. et al. Probing the transformation of boron nitride catalysts under oxidative dehydrogenation conditions. *J. Am. Chem. Soc.* **141**, 182–190 (2019).
- Lunsford, J. H. The catalytic oxidative coupling of methane. *Angew. Chem. Int. Ed.* **34**, 970–980 (1995).
- Lunsford, J. H. Catalytic conversion of methane to more useful chemicals and fuels: a challenge for the 21st century. *Catal. Today* **63**, 165–174 (2000).
- Qian, Q., Zhang, J., Cui, M. & Han, B. Synthesis of acetic acid via methanol hydrocarboxylation with CO₂ and H₂. *Nat. Commun.* **7**, 11481–11487 (2016).
- Kalck, P., Le Berre, C. & Serp, P. Recent advances in the methanol carbonylation reaction into acetic acid. *Coord. Chem. Rev.* **402**, 213078–213091 (2020).
- Barri, S. A. I. & Chadwick, D. Carbonylation of formaldehyde with zeolite catalysts. *Catal. Lett.* **141**, 749–753 (2011).
- Frank, B., Zhang, J., Blume, R., Schlögl, R. & Su, D. S. Heteroatoms increase the selectivity in oxidative dehydrogenation reactions on nanocarbons. *Angew. Chem. Int. Ed.* **48**, 6913–6917 (2009).
- Cheng, S. & Xu, B. Characterization of B₂O₃/ZrO₂ catalyst by ¹¹B MAS NMR. *Chin. J. Catal.* **25**, 393–396 (2004).
- Buyevskaya, O. V., Müller, D., Pitsch, I. & Baerns, M. Selective oxidative conversion of propane to olefins and oxygenates on boron-containing catalysts. *Stud. Surf. Sci. Catal.* **119**, 671–676 (1998).
- Hansen, M. R., Jakobsen, H. J. & Skibsted, J. Structural environments for boron and aluminum in alumina-borica catalysts and their precursors from ¹¹B and ²⁷Al single- and double-resonance MAS NMR experiments. *J. Phys. Chem. C* **112**, 7210–7222 (2008).
- Hu, Z. et al. Highly stable boron-modified hierarchical nanocrystalline ZSM-5 zeolite for the methanol to propylene reaction. *Catal. Sci. Technol.* **4**, 2891–2895 (2014).
- Dong, W. Y., Sun, Y. J., He, H. Y. & Long, Y. C. Synthesis and structural characterization of B-Al-ZSM-5 zeolite from boron-silicon porous glass in the vapor phase. *Micropor. Mesopor. Mater.* **32**, 93–100 (1999).
- Mansouri, S. et al. Partial oxidation of methane over modified Keggin-type polyoxotungstates. *J. Mol. Catal. A Chem.* **379**, 255–262 (2013).
- Zhang, J., Burklé-Vitzthum, V., Marquaire, P. M., Wild, G. & Commenge, J. M. Direct conversion of methane in formaldehyde at very short residence time. *Chem. Eng. Sci.* **66**, 6331–6340 (2011).
- Quintana-Solórzano, R., Barragán-Rodríguez, G., Armendáriz-Herrera, H., López-Nieto, J. M. & Valente, J. S. Understanding the kinetic behavior of a Mo-V-Te-Nb mixed oxide in the oxydehydrogenation of ethane. *Fuel* **138**, 15–26 (2014).
- García-Diéguez, M., Chin, Y. H. & Iglesia, E. Catalytic reactions of dioxygen with ethane and methane on platinum clusters: mechanistic connections, site requirements, and consequences of chemisorbed oxygen. *J. Catal.* **285**, 260–272 (2012).
- Chin, Y. H., Buda, C., Neurock, M. & Iglesia, E. Consequences of metal-oxide interconversion for C-H bond activation during CH₄ reactions on Pd catalysts. *J. Am. Chem. Soc.* **135**, 15425–15442 (2013).
- Barbero, J., Banares, M., Pena, M. & Fierro, J. Partial oxidation of methane into C₁-oxygenates: Role of homogeneous reactions and catalyst surface area. *Catal. Today* **71**, 11–19 (2001).

Acknowledgements

This work was supported by the National Natural Science Foundation of China (No. 21922201, 21872113, 91945301, 21673189, and 91545114) and the Fundamental Research Funds for the Central Universities (No. 20720190036 and 20720160032).

Author contributions

Shu.W. and Y.W. conceived the idea for the project. J.Ti., J.Ta., and M.Y. conducted the material synthesis. P.H., M.Y., and J.Ta. performed the structural characterizations and catalytic test. Sha.W., Y.W., J.L., and Z.Z. discussed the catalytic results. J.Ti. drafted the manuscript under the guidance of Y.W. and Shu.W. All authors discussed and commented on the manuscript.

Competing interests

The authors declare no competing interests.

Additional information

Supplementary information is available for this paper at <https://doi.org/10.1038/s41467-020-19517-y>.

Correspondence and requests for materials should be addressed to S.W. or Y.W.

Peer review information *Nature Communications* thanks the anonymous reviewer(s) for their contribution to the peer review of this work. Peer reviewer reports are available.

Reprints and permission information is available at <http://www.nature.com/reprints>

Publisher's note Springer Nature remains neutral with regard to jurisdictional claims in published maps and institutional affiliations.



Open Access This article is licensed under a Creative Commons Attribution 4.0 International License, which permits use, sharing, adaptation, distribution and reproduction in any medium or format, as long as you give appropriate credit to the original author(s) and the source, provide a link to the Creative Commons license, and indicate if changes were made. The images or other third party material in this article are included in the article's Creative Commons license, unless indicated otherwise in a credit line to the material. If material is not included in the article's Creative Commons license and your intended use is not permitted by statutory regulation or exceeds the permitted use, you will need to obtain permission directly from the copyright holder. To view a copy of this license, visit <http://creativecommons.org/licenses/by/4.0/>.

This is a U.S. government work and not under copyright protection in the U.S.; foreign copyright protection may apply 2020